Thesis-1985-P735m

Plummer, David Warren, 1962-

Page Number 72

- [x] Images
- [ ] Foldouts
- [ ] Maps

- [ ] Scanned
- [ ] Clean-up
- [ ] PDF

- [ ] Archive MSF
- [ ] Projects

ZS
Verified

8/25
Date

MODELING AND SENSITIVITY ANALYSIS OF THE REWIND PORTION OF A WEB HANDLING MACHINE

By

DAVID WARREN PLUMMER

Bachelor of Science

Oklahoma State University

Stillwater, Oklahoma

1984

Submitted to the Faculty of the Graduate College
of the Oklahoma State University
in partial fulfillment of the requirements
for the Degree of
MASTER OF SCIENCE
December, 1985

MODELING AND SENSITIVITY ANALYSIS

OF THE REWIND PORTION OF A

WEB HANDLING MACHINE

Thesis Approved:

Mary E. Young
Thesis Adviser

James K. Good

R. F. Lowery

Norman N. Durham
Dean of the Graduate College

ACKNOWLEDGMENTS

I would like to take this opportunity to acknowledge and express my sincere appreciation to my adviser, Dr. Gary E. Young, for his insight, guidance, and limitless patience. His influence on the outcome of this endeavor was invaluable. The input from Dr. Richard Lowery, Dr. Keith Good, and Dr. John Shelton was much needed and is greatly appreciated.

To my friend, Howard Conlon, I can only say "thank you" for your paramount influence on my outlook on life. My academic success stems from the attitudes and inspiration which you instilled in me as an undergraduate.

Many thanks to my family, Mary Beth, my fiancée, for making me feel it was all worthwhile; and my parents for giving me the opportunities they never had.

Last, but not least, I would like to acknowledge Charlene Fries for typing this manuscript so promptly under such a severe time constraint.

TABLE OF CONTENTS

LIST OF TABLES

LIST OF FIGURES

CHAPTER I

INTRODUCTION

The term "web" describes a thin strip of material which has negligible resistance to bending. A thin strip is one in which the length is much larger than the width and the width is several orders of magnitude greater than the thickness. Many household products are packaged in or sold as webs. The most common web products are paper, foil, film, and fabric. Most directly analogous to the types of webs studied in this report are the wrappers for food, such as candy bars and potato chips.

Many materials, in spite of their final state, are at one time handled in a web form. For example, flat sheets of asbestos are rolled to form pipe and tubing. The advantage to processing in this manner is its efficiency and savings in time. Webs can be handled in a continuous fashion rather than in discrete pieces. Consider the publishing and printing industry which previously used flat plate printing. Now almost all printing is done by rotary printers which operate at high speeds. Much of the technology in web handling comes from the paper and pulp industry. It is not uncommon for machines which handle other forms of webs, such as film or fabric, to be converted paper machines.

Due to the continuous nature of webs, they are typically handled in rolls or spools. Therefore, winding and unwinding are major operations in web handling. In the interest of efficiency, these processes are done at high speeds. As with any high speed rotary equipment, special problems

exist with the dynamic response. These problems manifest themselves in various forms. Some cause vibration or chattering of the winding equipment while others affect the web directly. These web effects include a starred or buckled region inside the core of the roll, permanent stretch marks and wrinkles, hard lumps or bulges in the roll, known as gage band defects, and telescoping.

Although the exact causes of these problems are not known, they can generally be divided into two categories: winding machine effects and wound roll effects. Eccentricities of the cores, roller alignment, characteristic frequencies of the machine and fluctuations in web tension are common winding machine effects. Wound roll effects include resonances in thickness variation, air entrainment, and limited interlayer friction.

Web winding machines have been designed to deal with the problems mentioned above. Two types of winding machines are the center driven-riding roll winder and the surface driven winder. Both of these machines utilize the contact or nip pressure between a drum or roller and the wound roll to limit air entrainment. A device on many winders used to control on-line longitudinal tension is known as a dancer. The dancer can be a passive device which moves about a static equilibrium position in response to fluctuations in web tension or be a part of a tension control system including braking and input torque control. The design and control of these winding machines is constrained by a lack of true understanding of the mechanics involved in winding and web handling in general.

An extensive literature search was conducted using dial-on computer libraries and engineering references. The results of these searches revealed an important reason for the lack of understanding of web handling.

Little quantitative work has been conducted in this important area of manufacturing and processing. TAPPI, the technical journal of the paper and pulp industry, contains several informative entires on the winding process. However, these works are qualitative in nature. Since the conclusions of these papers are commonly drawn on empirical evidence, they serve to provide background information and inspire topics for future analytical and theoretical research. Many of these papers provide a good source of experimental data which can be used to check the performance of a model simulation.

A limited amount of analytical work has been published in the last 15 years. In 1968, Altmann [1] published formulas for computing stresses in center-wound rolls. Two important equations were presented. The first expresses the interface pressure and the second relates the in-roll tension stress as a function of winding tension stress, radius ratio, and elastic properties of the web.

Later in 1968, Shelton [2] published his thesis which dealt with lateral dynamics and stability of webs. This thesis spawned two works by Shelton and Reid [3, 4]. The first offered a simplified dynamic analysis of a moving web neglecting the material properties. The second presents a second-order method used for systematic derivation of ordinary differential equations describing the lateral dynamic behavior of massless, moving webs.

Another dissertation presenting analytical work was published in 1974 by Blaedel [5]. Blaedel considered the winding of a roll of paper as a design problem in which a mathematical model of the roll structure was developed and applied to a surface driven winder. Also, system equations were derived which could be used to control the winding process.

Soong and Li [6] in 1979 extended the work published by Shelton and Reid by performing an elastic analysis of multi-roll endless web systems. Problems concerning edge guide force, steering moment, pivoting cylinders, and other parameters were analyzed.

The most recent publication uncovered by the literature search was written by Veits, Beilin, and Merkin [7] in 1983. Analysis was performed on elastic strips of web which were modeled as a flexible plate under the action of longitudinal tensile forces. The validity of a one-dimensional model for the elastic strip is also examined.

An important problem not yet considered in the area of web handling is determining the effect of tension control on the winding process. Tension control is important because the on-line tension directly affects air entrainment, buckling of the web core, wrinkling, yielding, and stretching of the web. All of these phenomena are important to the final quality of the wound roll.

It is the objective of this thesis to quantitatively determine the controlling parameters in obtaining an acceptable response in a web winding system. The analysis which follows will focus on the rewind portion of a "typical" center driven-rider roll winding machine. Actually, the field of web handling is so diverse that a typical winding machine does not exist. However, all winding machines share certain common elements, such as a web, rewind rolls, and some type of device for tension control. The methods presented in this thesis are directly applicable to any center driven-rider roll winding machine.

To accomplish the above task, it will be necessary to construct a detailed mathematical model of the dancer, the rewind roll, and the controlling feedback system. The continuous nature of the web must also be

included in the model. The most influential parameters of the model can be identified through a sensitivity analysis. The type of analysis to be employed in this thesis is presented by Hornberger and Spear [8]. The particular method offers several advantages over the classical Bode sensitivity technique. The Hornberger and Spear method is: (1) easy to apply to nonlinear system, (2) dependent on the range of a parameter and not a point value, and (3) not directly affected by the number of unknown parameters.

Chapter I of this thesis has provided some definitions of terms used in web handling and presented the objective of the work that follows. Chapters II and III deal with the development and analysis of a continuous and discrete model of the web and dancer on a center driven-rider roll winding machine. The sensitivity analysis of the model is presented in Chapter IV. Conclusions and recommendations appear in Chapter V.

CHAPTER II

SYSTEM DESCRIPTION

In the investigation of physical problems, mathematical modeling is essential. It is common practice to approximate certain processes or elements of the actual system with components whose scientific descriptions are well known. The measures for the value of a model are its ability to accurately describe the system it represents and its compliance to mathematical manipulation.

2.1 Component Descriptions

The analysis conducted in this thesis applies to a center driven-rider roll (CDRR) winding machine as shown in Figure 1. The vector $\underline{V}$ shows the direction of the moving web during the winding process. The terms lateral, longitudinal, and normal will be used often in the following text. Figure 2 clarifies the meaning of these terms.

All of the elements shown in Figure 1 are connected by flexible free spans of the web. Since the thickness of the web is much smaller than the width and span length, the web has little resistance to torsion or bending about the lateral axis. However, the web will resist a moment about the normal axis. This resistance allows for in-plane steering of the web by changing the alignment of the rollers.

The dancer is a tension controlling device which can passively respond to variations in longitudinal tension or can be part of a control

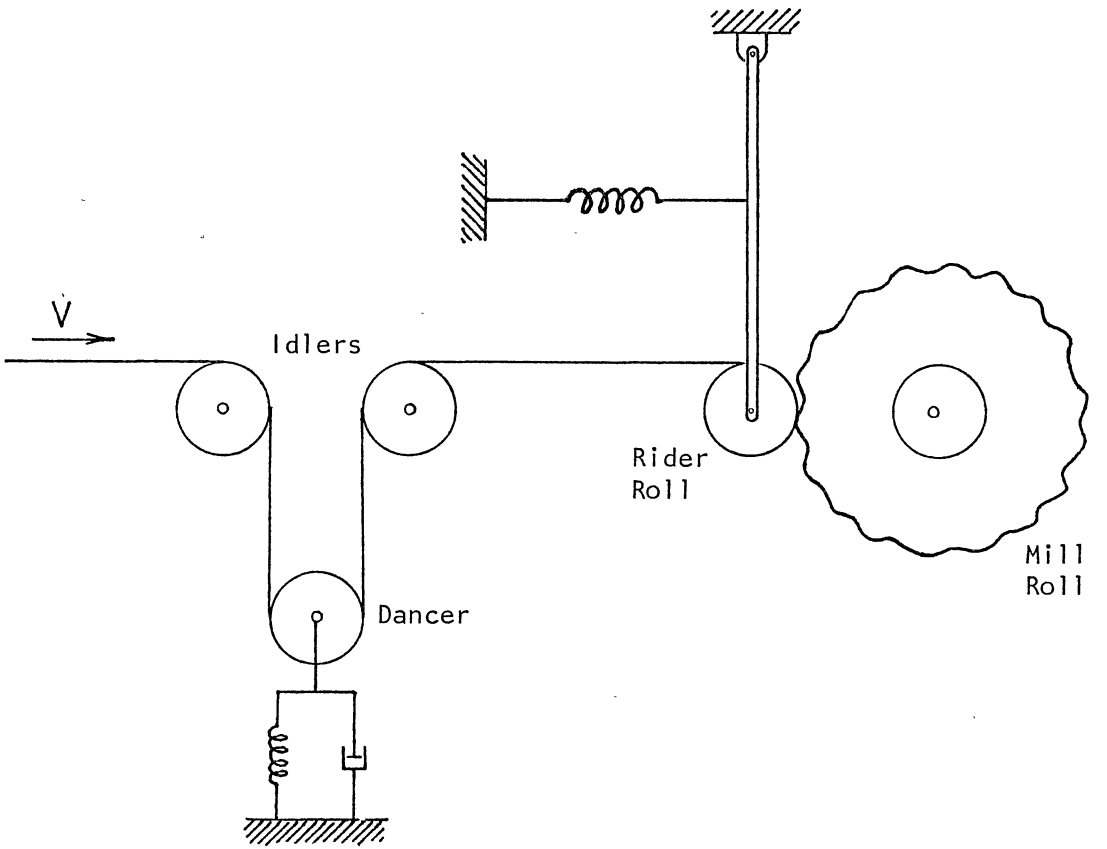

Figure 1. Schematic Drawing of the Rewind Portion of a Center-Driven-Rider Roll Winding Machine

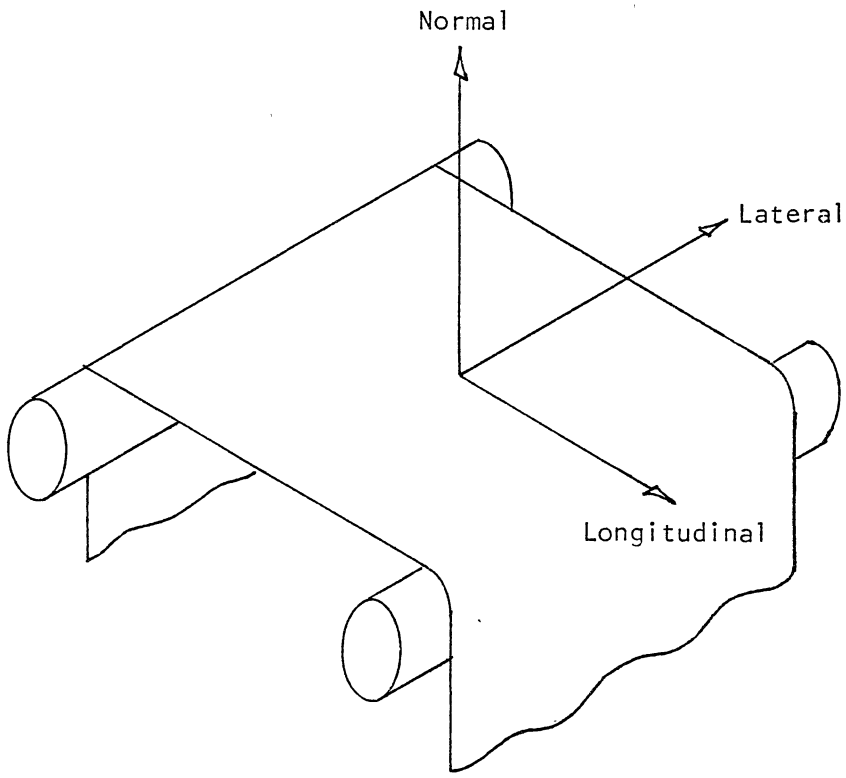

Figure 2. Definition of Web Directions

system. Physically, the dancer is a roller which is elastically supported. As a passive device, the dancer moves up and down to keep the web taut. When tension in the web decreases, the spring pulls the dancer down until the slack in the web is exhausted. The dancer can also be used as a tension sensor. The position of the dancer can be used to control the input torque applied at the center of the mill roll. For example, when the web is slack, the dancer will move down. A signal, indicating both the sense and magnitude of the dancer motion, sent to the motor can increase the input torque accordingly to take up the excess web.

The mill roll consists of windings of web about a spool of metal, plastic, cardboard, or similar material. Ideally, the mill roll is homogeneous with a circular cross section. However, variations in thickness, stretching, and air entrainment create problems such as starring (Figure 3) and gage bands (Figure 4). Excessive air entrainment can even cause some of the windings to droop when the mill roll is not rotating.

The rider roll is simply a follower on a cam which is held in place by the tension of a pneumatic spring. The rider serves to limit air entrainment and to insure smooth rolls. The rider roll is mounted on a pivot which is part of a sled connected to the frame of the winder. As the diameter of the mill roll increases, the sled moves backward which allows the rider roll arm to remain approximately vertical. During ideal operating conditions, the rider roll is in constant contact with the mill roll. The rotation of the rider roll arm is quasi-static, changing only with the gradual increase in diameter of the mill roll.

2.2 The Model and Assumptions

Viets, Beilin, and Merkin [7] investigated an elastic strip in

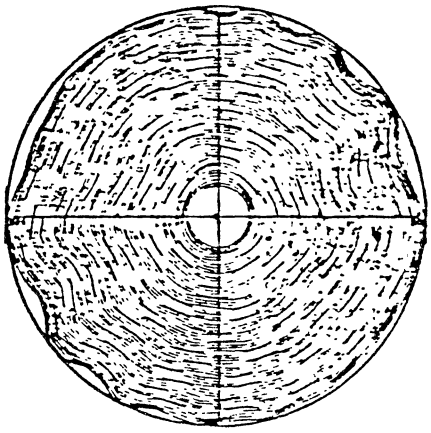

Figure 3. Starring Defect in the Mill Roll

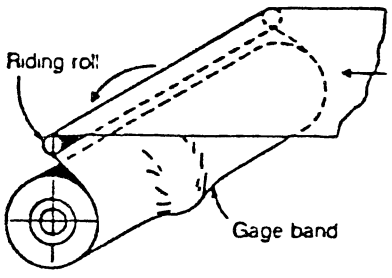

Figure 4. Gage Band Defect in the Mill Roll

mechanisms with flexible coupling. Their approach was a comparison to general solutions of the planar oscillations of plates on strips of web. For free longitudinal oscillations, comparison of the first eigenfrequencies of a two-dimensional and rod model found that the difference was less than 1 percent. Viets et al. determined that for longitudinal oscillations, the use of one-dimensional models for the purpose of simplification was expedient even with a large relative strip width and Poisson's ratio of the strip material.

If the assumptions are made that the oscillations of the web remain in plane, the centerline of the web moves along the longitudinal axis, and the web is straight, uniform, and uncambered, then it is reasonable to employ a one-dimensional representation of the web. The appropriate one-dimensional model for the web is the axial rod. The rod will permit tension to vary along the length which supports axial vibration but offers no resistance to bending about any axis. Since the actual web will resist a moment about the normal axis, it is necessary to assume that the rollers have parallel alignment and deflections in the lateral direction are nonexistent.

The dancer is a heavy flywheel which is supported via a pneumatic spring and rotates at a rate proportional to the line speed of the web. The dancer is constrained to translate in one direction only. Thus, there will be no gyroscopic effects if both ends of the dancer move together. This is equivalent to stating that no rotation can occur about the longitudinal axis. Without rotary properties, the dancer reduces to an elastically supported point mass.

Figure 5 shows the model which is equivalent to the web and dancer. The forcing function, $f(t)$, is a displacement input to the web span

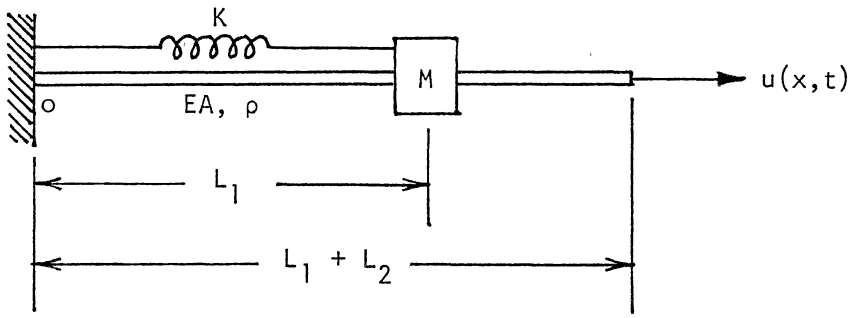

Figure 5. One-Dimensional Representation of the Dancer and Web

representing any relative change in the mill roll radius from the nominal value. Ideally, f(t) would be zero for all time. However, eccentricities in the core and starring of the windings in the mill roll can account for a nonzero displacement input. The forcing function, f(t), is of the form

$$f(t) = r - \sqrt{r^2 + e^2 + 2er \cos \omega t} - N \cos n \omega t \qquad (2.1)$$

where

r = mill roll radius;

e = eccentricity of the mill roll core;

ω = rotational speed of the mill roll;

n = number of nodes on the star inside the mill roll; and

N = amplitude of the mill roll stars.

Notice that all of the idlers and the rider roll have been omitted from the model. The idlers have no contribution because they are fixed in space and can only rotate about their own lateral axis. The coefficient of friction is assumed to be small between the web and rollers. For this reason, it is assumed that the rotation of the idlers and rider roll have no effect on the moving web.

The rods shown in Figure 5 have axial stiffness, EA, and mass per unit length, ρ, which correspond to the same properties of the web. The block has the same mass as the dancer while the elastic element, K, has the same properties as the pneumatic spring, linearized about its nominal position. The rods are grounded at one end because personal observation of winding machines has shown that web disturbances propagate a finite distance upstream from the winding apparatus.

2.3 Justifications of Assumptions

The model for the web and dancer was presented in the previous section. Several assumptions were made in the development of the model. These assumptions should be examined further to determine if any important aspects of the problems have been omitted.

The foremost assumption is that the two-dimensional web can be examined as a rod. This assumption entails that the web be straight and uniform. This is never true in the strictest sense. However, since the thickness is several orders of magnitude smaller than the width and length, small variations in this thickness are negligible to the dynamic properties of the web. These same variations in thickness are important in examining the internal structure of the mill roll, which is beyond the scope of this thesis. To treat the web as a rod, it is also necessary to require that the gradient of lateral tension is zero. A lateral gradient would arise from misalignment of rollers. It seems reasonable to assume that with care proper alignment of the rollers is possible. The causes and effects of lateral tension gradients will be investigated in future works.

The rotary effects of the rider roll and idlers was neglected. This assumption implies that the rotary inertia sees no acceleration and that no gyroscopic effects are induced. Except during start up or shut down, the handling operations for the web typically occur at constant line speed. Thus, for a steady state operation, the rollers would not accelerate. However, longitudinal fluctuations in the web give rise to instantaneous changes in the velocity of the web at any point along the span. The broad flat surface of the web traveling through open expanses of air

acts as a plate of a large capacitor which collects a static charge. This static charge suspends a thin film of air against the face of the web which practically negates any frictional effects between the web and the rollers. This allows the web to accelerate freely with little interaction with the rollers.

A displacement input, f(t), is applied to the free end of the rod. This input function accounts for the effects of the mill roll defects on the web. The causes and exact nature of mill roll defects have not been investigated. No attempt will be made in this thesis to accurately explain these defects. They must, however, be included in any model of a web winding system. Thus, the mill roll defects are assumed to be an inherent part of the system like the web density or the modulus of elasticity.

CHAPTER III

MATHEMATICAL MODEL OF A WINDING MACHINE

The model to be analyzed is shown in Figure 5. The first step in the analysis ofany vibration problem with linear constant coefficients is the solution of the eigenvalue problem. This solution yields the characteristic frequencies and the mode shapes. The characteristic frequencies are a measure of the speed at which free motion occurs. The mode shapes contain the corresponding spatial information for free motion. Using the eigenvalue information, it is possible to obtain the solution by superimposing the mode shapes and the corresponding time functions.

3.1 The Eigenvalue Problem

The motion of the web, which is assumed to behave as a rod, is governed by the wave equation. Because of the concentrated mass and spring in the midspan of the rod, it is convenient to replace the overall system by two subsystems. Figure 6 shows these subsystems and the coordinates used to describe their motion. The forcing function is omitted from the analysis because the eigenvalue problem deals with systems in free motion. The preliminary analysis of both subsystems is identical. The analysis will be performed in detail on subsystem A with the tacit understanding that equivalent operations are to be applied to subsystem B.

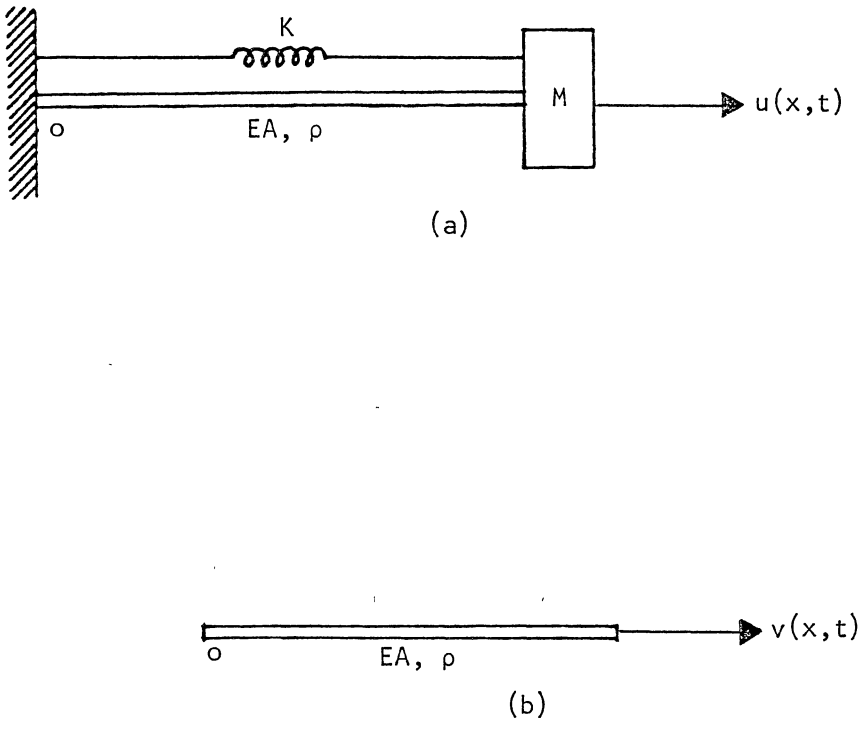

Figure 6. Subsystems of Web and Dancer Model With Coordinates

The wave equation for a uniform, homogeneous rod in axial vibration is

$$\rho \frac{\partial^2 u}{\partial t^2} dx - EA \frac{\partial^2 u}{\partial x^2} dx = 0 \tag{3.1}$$

where

E = modulus of elasticity;

A = cross-sectional area; and

ρ = mass per unit length.

This is a two-dimensional partial differential equation. The classic approach to solving this type of equation is to assume that the function which satisfies the above equation can be separated into a function of time and a function of space only. Thus,

$$u(x,t) = w(x)\ h(t), \qquad \text{for } 0 \leq x \leq (L_1 + L_2) \tag{3.2}$$

Performing the required partial derivatives and substituting into Equation (3.1) yields

$$\rho w(x)\ \ddot{h}(t)\ dx - EA\ w''(x)\ h(t)\ dx = 0 \tag{3.3}$$

where

$$\ddot{h}(t) = \frac{d^2 h}{dt^2}$$

and

$$w''(x) = \frac{d^2 w}{dx^2}$$

Dividing by $\rho w(x)\ h(t)$ and defining a^2 as follows reveals that

$$a^2 = \frac{EA}{\rho} \tag{3.4}$$

$$\frac{\ddot{h}(t)}{h(t)} = a^2 \frac{w''(x)}{w(x)} \tag{3.5}$$

The left side of Equation (3.5) is a function of time only, while the right side is a function of space only. This implies that both equations must equal a constant. Denoting this arbitrary constant as $-\omega^2$ yields two independent second-order differential equations:

$$\ddot{h}(t) = -\omega^2 h(t) \tag{3.6}$$

$$w''(x) + \frac{\omega^2}{a^2} w(x) = 0 \tag{3.7}$$

The solution of Equation (3.7) is

$$w(x) = C_1 \sin \frac{\omega}{a} x + C_2 \cos \frac{\omega}{a} x \tag{3.8}$$

where C_1 and C_2 are arbitrary constants to be determined from the boundary conditions. The corresponding equations for subsystem B are

$$v(x,t) = y(x)\ \xi(t), \qquad \text{for } L_1 \le x \le L_2 \tag{3.9a}$$

$$\ddot{\xi}(t) = -\Omega^2 \xi(t) \tag{3.9b}$$

$$y''(x) + \frac{\Omega^2}{a^2} y(x) = 0 \tag{3.9c}$$

$$y(x) = D_1 \sin \frac{\Omega}{a} x + D_2 \cos \frac{\Omega}{a} x \tag{3.9d}$$

The boundary conditions for this problem are

$$u(o,t) = 0 \tag{3.10a}$$

$$v(L_1 + L_2,\ t) = 0 \tag{3.10b}$$

$$u(L_1,\ t) = v(L_1,\ t) \tag{3.10c}$$

$$EA\left[\frac{\partial u}{\partial x}(L_1, t) - \frac{\partial v}{\partial x}(L_1, t)\right] = -M \frac{\partial^2 u}{\partial t^2}(L_1, t) - K\, u(L_1, t) \tag{3.10d}$$

Using Equations (3.2), (3.6), and (3.9), the boundary conditions become

$$w(o) = 0 \tag{3.11}$$

$$y(L_1 + L_2) = 0 \tag{3.12}$$

$$w(L_1) = y(L_1) \tag{3.13}$$

$$EA[w'(L_1) - y'(L_1)] = (M\omega^2 - K)\, w(L_1) \tag{3.14}$$

Substituting Equation (3.11), Equation (3.8) becomes

$$w(x) = C_1 \sin \frac{\omega}{a} x \tag{3.15}$$

Expansion of Equation (3.12) reveals that

$$C_1 = D_1 + D_2 \cot \frac{\omega L_1}{a} \tag{3.16}$$

Substitution into Equations (3.13) and (3.14) yields

$$EA\left[\frac{\omega}{a}(D_1 - C_1) \cos \frac{\omega L_1}{a} - \frac{D_2 \omega}{a} \sin \frac{\omega L_1}{a}\right]$$

$$= (K - M\omega^2)\, C_1 \sin \frac{\omega L_1}{a} \tag{3.17}$$

$$D_1 \sin \frac{\omega(L_1 + L_2)}{a} + D_2 \cos \frac{\omega(L_1 + L_2)}{a} = 0 \tag{3.18}$$

Combining Equations (3.16) through (3.18) yields the following matrix equation:

$$\begin{bmatrix} \sin^2 \frac{\omega L_1}{a} & \cos \frac{\omega L_1}{a} \sin \frac{\omega L_1}{a} + \frac{EA\,\omega}{a(K - M\omega^2)} \\ \sin \frac{\omega(L_1 + L_2)}{a} & \cos \frac{\omega(L_1 + L_2)}{a} \end{bmatrix} \begin{Bmatrix} D_1 \\ D_2 \end{Bmatrix} = \begin{Bmatrix} 0 \\ 0 \end{Bmatrix} \tag{3.19}$$

The only nontrivial solution to Equation (3.19) is for the determinant to be nonzero. Thus,

$$\sin \frac{\omega L_1}{a} \sin \frac{\omega L_2}{a} + \frac{EA\,\omega}{a(K - M\omega^2)} \sin \frac{\omega(L_1 + L_2)}{a} = 0 \qquad (3.20)$$

Equation (3.20) is a transcendental equation which can only be solved numerically. Note that a singularity exists at the undamped natural frequency of the dancer mass and spring acting as an independent single-degree-of-freedom system. This frequency corresponds to

$$\omega = \sqrt{\frac{K}{M}} \qquad (3.21)$$

It is also interesting to note that Equation (3.20) is satisfied for $\omega = 0$. This frequency represents column buckling and is meaningless for this application.

3.2 Analysis of Subsystems

In the solution of continuous vibration problems, it is possible to use the orthogonality ofthe eigenfunctions to find a set of principal coordinates. Principal coordinates allow for the spatial and dynamic information to be separated.

3.2.1 Eigenvalue Analysis of Subsystem A

Figure 7(a) shows subsystem A which is excited by $g_1(t)$. This function represents the effect of subsystem B on subsystem A and also describes the motion of the concentrated mass. Analysis of subsystem A now becomes a support motion problem with eigenvalues on the boundary.

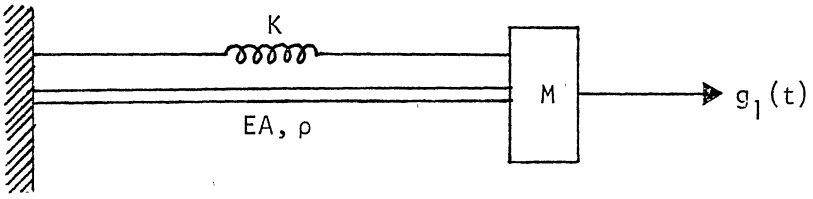

(a)

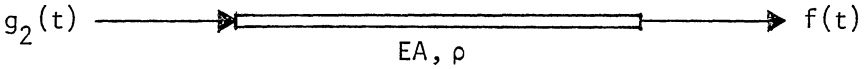

Figure 7. Subsystems of Web and Dancer Model With Forcing Function

Timoshenko, Young, and Weaver [9] treat problems of this nature by dividing the total motion into two parts:

$$u(x,t) = u_{st} + u^* \tag{3.22}$$

In the above expression the symbol u_{st} denotes the displacement of any point on a massless bar due to support motion. Such a function is determined by static analysis to be

$$u_{st}(x,t) = \frac{x}{L_1} g_1(t) \tag{3.23}$$

This part of the displacement is generalized as the flexible-body motion of a massless rod. The symbol u^* represents the displacement of any point on the rod relative to u_{st}. Thus, the relative motion u^* will be associated with the inertial forces distributed over the length of the bar. Substituting Equation (3.22) into Equation (3.1) and using Equation (3.23) yields

$$\rho \frac{\partial^2 u^*}{\partial t^2} dx - EA \frac{\partial^2 u^*}{\partial x^2} dx = -\rho \frac{\partial^2 u_{st}}{\partial t^2} dx \tag{3.24}$$

Since eigenvalues are a measure of free response, the forcing function is set to zero. Thus, Equation (3.24) is now identical to Equation (3.3). Separation of time and spatial components can be achieved by assuming that

$$u^*(x,t) = \phi(x)\, q(t) \tag{3.25}$$

It follows from the boundary conditions that

$$\phi(x) = C_1 \sin \frac{\omega}{a} x \tag{3.26}$$

The boundary condition at the concentrated mass is

$$EA\ \phi'(L_1) = (M\omega^2 - K)\ \phi(L_1) \tag{3.27}$$

Substitution for $\phi(L_1)$ and $\phi'(L_1)$ from Equation (3.26) leads to

$$\tan \frac{\omega L_1}{a} = \frac{EA\,\omega}{a(M\omega^2 - K)} \tag{3.28}$$

Equation (3.28) is a transcendental equation which can be solved for an infinite number of eigenvalues. Limiting the focus on the first eigenvalue and assuming that $a >> \omega_1 L_1$, then

$$\omega_1 = \sqrt{\frac{K}{M} + \frac{EA}{ML_1}} \tag{3.29}$$

It is interesting to note that the first eigenfrequency is independent of the mass of the rod. Equation (3.28) shows that the rod acts as a massless spring of stiffness EA/L_1 for all modes of vibration where the assumption of $a >> \omega_i L_1$ is valid.

3.2.2 Orthogonality Conditions for Subsystem A

In order to develop the orthogonality relationships, the eigenvalue problem must be written for two distinct modes. For the sake of brevity, manipulations will be performed on the ith mode, while the corresponding operations on the jth mode will be omitted from the text. The eigenvalue problem for the ith mode is

$$EA\ \phi_i'' = -\rho\omega_i^2\ \phi_i \tag{3.30}$$

Multiplication of Equation (3.29) by ϕ_j and integration over the domain, $D_1:\{0 \le x \le L_1\}$, yields

$$EA \int_{D_1} \phi_i''\phi_j\, dx = -\rho\omega_i^2 \int_{D_1} \phi_i\phi_j\, dx \tag{3.31}$$

The concentrated mass and spring located at the free end of the rod must also be included in the orthogonality relationships. Equation (3.27) may be written as

$$EA\ \phi_i'(L_1)\ \phi_j(L_1) = (M\omega_i^2 - K)\ \phi_i(L_1)\ \phi_j(L_1) \tag{3.32}$$

Subtraction of Equation (3.32) from Equation (3.31) leads to

$$\begin{aligned} EA[&\int_{D_1} \phi_i''\phi_j\ dx - \phi_i'(L_1)\ \phi_j(L_1)] \\ &= \rho\omega_i^2 \int_{D_1} \phi_i\phi_j\ dx \\ &\quad - (M\omega_i^2 - K)\ \phi_i(L_1)\ \phi_j(L_1) \end{aligned} \tag{3.33}$$

The integral on the left-hand side of Equation (3.33) can be evaluated by parts. Thus,

$$\begin{aligned} EA[&\phi_i'(o)\ \phi_j(o) + \int_{D_1} \phi_i'\phi_j'\ dx] \\ &= \rho\omega_i^2 \int_{D_1} \phi_i\phi_j\ dx \\ &\quad + (M\omega_i^2 - K)\ \phi_i(L_1)\ \phi_j(L_1) \end{aligned} \tag{3.34}$$

Performing the same operations on the jth mode yields

$$\begin{aligned} EA[&\phi_i(o)\ \phi_j'(o) + \int_{D_1} \phi_i'\phi_j'\ dx] \\ &= \rho\omega_j^2 \int_{D_1} \phi_i\phi_j\ dx \\ &\quad + (M\omega_j^2 - K)\ \phi_i(L_1)\ \phi_j(L_1) \end{aligned} \tag{3.35}$$

Subtracting Equation (3.35) from Equation (3.34) and noting that $\phi_i(o) = \phi_j(o) = 0$, the following relation is obtained:

$$(\omega_i^2 - \omega_j^2)\left[\rho\int_{D_1} \phi_i\phi_j \, dx + M\,\phi_i(L_1)\,\phi_j(L_1)\right] = 0 \tag{3.36}$$

For the case when i = j, the above equation is identically satisfied. Thus, the bracketed term may equal any arbitrary constant, which will be denoted by m:

$$\rho\int_{D_1} \phi_i^2 \, dx + M\,\phi_i^2(L_1) = m \tag{3.37}$$

If the eigenfunctions are normalized such that the constant m is of the same magnitude as ρ, then Equations (3.33) and (3.34) become

$$EA[\phi_i'(L_1)\,\phi_i(L_1) - \int_{D_1} \phi_i''\phi_i \, dx] = EA\int_{D_1} (\phi_i')^2 \, dx$$

$$= M\omega_i^2 - K\phi_i^2(L_1) \tag{3.38}$$

3.2.3 Equations of Motion for Subsystem A

The equations of motion for subsystem A can be developed by recalling Equation (3.25):

$$\rho \frac{\partial^2 u^*}{\partial t^2} dx - EA \frac{\partial^2 u}{\partial x^2} dx = -\rho \frac{\partial^2 u_{st}}{\partial t^2} dx$$

The boundary condition at the free end of the bar is

$$M \frac{\partial^2 u^*}{\partial t^2}(L_1,t) + EA \frac{\partial^2 u^*}{\partial x^2}(L_1,t) + Ku^*(L_1,t) = 0 \tag{3.39}$$

Using the definition of u^*, multiplying by ϕ_j, and integrating over the domain, Equation (3.39) becomes

$$\rho\ddot{q}_1 \int_{D_1} \phi_i\phi_j \, dx - EA\, q_i \int_{D_1} \phi_i''\phi_j \, dx = -\rho\int_{D_1} \frac{\partial^2 u_{st}}{\partial t^2} \phi_j \, dx$$

(3.40)

The boundary condition, Equation (3.39), can be transformed using Equation (3.25) to

$$M\ddot{q}_i(t)\ \phi_i(L_1) + EA\ q_i(t)\ \phi_i''(L_1) + K\ q_i(t)\ \phi_i(L_1) = 0 \tag{3.41}$$

Multiplication of Equation (3.41) by $\phi_j(L_1)$ and addition of Equations (3.40) and (3.41) yields

$$\begin{aligned}[\rho\int_{D_1} \phi_i\phi_j\ dx + M\ \phi_i(L_1)\ \phi_j(L_1)]\ \ddot{q}_i(t) \\ + K\ \phi_i(L_1)\ \phi_j(L_1)\ q_i(t) \\ - EA[\int_{D_1} \phi_i''\phi_j\ dx - \phi_i'(L_1)\ \phi_j(L_1)]\ q_i(t) \\ = -\rho\int_{D_1} \frac{\partial^2 u_{st}}{\partial t^2}\ \phi_j\ dx\end{aligned} \tag{3.42}$$

Using Equations (3.37) and (3.38) when i = j, Equation (3.42) becomes

$$m(\ddot{q}_i + \omega_i^2\ q_i) = -\rho\int_{D_1} \frac{\partial^2 u_{st}}{\partial t^2}\ \phi_i\ dx$$

But m is equal in magnitude to ρ, so

$$\ddot{q}_i + \omega_i^2\ q_i = -\int_{D_1} \frac{\partial^2 u_{st}}{\partial t^2}\ \phi_i\ dx \tag{3.43}$$

3.2.4 Analysis of Subsystem B

Figure 7(b) shows that subsystem B is a rod subjected to independent translations of both of its ends. However, the solution to the eigenvalue problem is obtained from an unforced system. Thus, subsystem

B is simply a rod with both ends free. The eigenfrequencies in Equation (3.9) are found by Meirovitch [10] to be

$$\Omega_i = \frac{i\pi a}{L_2}, \qquad i = 0.\ 1,\ 2,\ \ldots \tag{3.44}$$

and the eigenfunctions are

$$y(x) = D_i \cos \frac{\Omega_i}{a} x \tag{3.45}$$

To develop the orthogonality condition, it will again be advantageous to consider the absolute displacement as the sum

$$v(x,t) = v_{st} + v^* \tag{3.46}$$

where v_{st} and v^* are defined similarly to u_{st} and u^*, respectively. Since both ends of subsystem B translate, the static analysis yields

$$v_{st}(x,t) = \frac{L_2 - x}{L_2} g_2(t) + \frac{x}{L_2} f(t) \tag{3.47}$$

The general equation describing the motion of the rod can be written as

$$\rho \frac{\partial^2 v^*}{\partial t^2} dx - EA \frac{\partial^2 v^*}{\partial x^2} dx = -\rho \frac{\partial^2 v_{st}}{\partial t^2} dx \tag{3.48}$$

The space and time components of the relative motion can be separated by letting

$$v^*(x,t) = \psi_i(x)\ p_i(t) \tag{3.49}$$

Equation (3.48) can be rewritten using Equation (3.49) as

$$\psi_i(x)\ \ddot{p}_i(t) - a^2\ \psi_i''(x)\ p_i(t) = -\rho \frac{\partial^2 v_{st}}{\partial t^2} dx \tag{3.50}$$

where a is defined in Equation (3.4). Multiplying by and integrating over the domain, D_2:{$0 \le x \le L_2$}, yields

$$\ddot{p}_i(t) \int_{D_2} \psi_i \psi_j \, dx - a^2 p_i(t) \int_{D_2} \psi_i'' \psi_j \, dx = -\int_{D_2} \frac{\partial^2 v_{st}}{\partial t^2} \psi_j \, dx \tag{3.51}$$

To obtain equations of motion, interest is focused on the case where i = j. Equation (3.51) becomes

$$\ddot{p}_i(t) \int_{D_2} \psi_i^2 \, dx - a^2 p_i(t) \int_{D_2} \psi_i'' \psi_i \, dx = -\int_{D_2} \frac{\partial^2 v_{st}}{\partial t^2} \psi_i \, dx \tag{3.52}$$

From Equation (3.45), it is clear that

$$\psi_i(x) = -\frac{\Omega_i^2}{a^2} \psi_i(x) \tag{3.53}$$

Equation (3.45) can be normalized such that

$$\int_{D_2} \psi_i^2(x) \, dx = 1$$

Thus, Equation (3.52) becomes

$$\ddot{p}_i + \Omega_i^2 p_i = -\int_{D_2} \frac{\partial^2 v_{st}}{\partial t^2} \psi_i \, dx \tag{3.54}$$

3.2.5 Combining the Subsystems

Using Equations (3.24) and (3.47), the principal equations of motion (3.43) and (3.54) can be rewritten as

$$\ddot{q}_i + \omega_i^2 q_i = -\frac{\ddot{g}_1(t)}{L_1} \int_{D_1} x \phi_i \, dx \tag{3.55}$$

$$\ddot{p}_i + \Omega_i^2 p_i = \frac{\ddot{g}_2(t)}{L_2} \int_{D_2} (x - L_2) \psi_i \, dx$$

$$- \frac{\ddot{f}(t)}{L_2} \int_{D_2} x \psi_i \, dx \tag{3.56}$$

Continuity of the rods dictates that $g_1(t) = g_2(t) = g(t)$. Equations (3.55) and (3.56) are expressed in terms of three unknowns. The third equation necessary for a solution comes from applying Newton's Second Law to the mass, whose motion is g(t):

$$M\ddot{g}(t) + Kg(t) = EA[\frac{\partial u^*}{\partial x}(L_1) + \frac{\partial v^*}{\partial x}(o)] \tag{3.57}$$

Equation (3.57) becomes the third equation of motion if the definitions for u^* and v^* are substituted:

$$M\ddot{g}(t) + Kg(t) = EA[\phi_i'(L_1) \, q_i(t) + \psi_i'(o) \, p_i(t)] \tag{3.58}$$

Equations (3.55), (3.56), and (3.58) can provide the equations of motion for as many modes of vibration as desired. Equation (3.55) can be written for $q_1, q_2, \ldots, q_n$, while Equation (3.56) can be written for $p_1, p_2, \ldots, p_n$. Equation (3.58) is written only one time but the right-hand side becomes the summation of $\phi_i'(L_1) \, q_i(t)$ and $\psi_i'(o) \, p_i(t)$. This This procedure will always result in 2n+1 equations in 2n+1 unknowns.

3.3 Discrete Model of the System

The solution to the equations of motion developed in the previous section allows for prediction of any point on the web as a function of time. However, the main goal of modeling this system was to predict

dancer motion and improve tension control. Since the mass of the web is small compared to the mass of the dancer, it may be possible to neglect the inertial effects of the web. Without inertia, the web behaves as a spring of stiffness EA/L. The partial differential equations reduce to a single, second-order differential equation.

The advantages of a discrete model over the continuous model developed above are: the equations of motion are easier to manipulate, damping can be more easily considered, and nonlinear effects can be included. The major disadvantage to a discrete model is that the information is lost in neglecting the higher modes of vibration of the web.

A discrete model for the system is shown in Figure 8. The web is represented by its elastic properties only. From Newton's Second Law, the governing equation of motion is

$$M\ddot{x} + \left(K + \frac{EA}{L_1} + \frac{EA}{L_2}\right)x = \frac{EA}{L_2} f(t) \tag{3.59}$$

where f(t) is the displacement input expressed by Equation (2.1). The natural frequency of the model as predicted by Equation (3.59) is

$$\omega_1 = \sqrt{\frac{K}{M} + \frac{EA}{ML_1} + \frac{EA}{ML_2}} \tag{3.60}$$

At the nominal conditions which are discussed in Chapter III, the first nonzero solution of Equation (3.20) is $\omega_1 = 17.89\ s^{-1}$ and evaluating Equation (3.60) with the nominal values yields $\omega_1 = 17.70\ s^{-1}$. This is approximately a 1 percent difference between the fundamental frequencies predicted by the two models.

Correlation of the first natural frequencies is not sufficient cause to abandon the continuous model in favor of the discrete one.

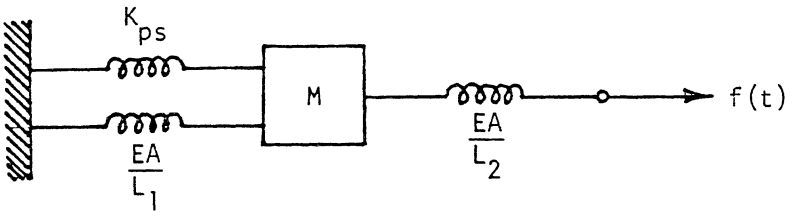

Figure 8. Discrete Model of Web and Dancer System

However, this agreement does encourage further investigation of the discrete model. Since the motion of the dancer is related to the longitudinal tension, the deciding comparison should be the amplitude of the dancer motion.

Equations (3.55), (3.56), and (3.58) can be solved analytically for the first mode if f(t) is a well-behaved function. Equation (2.1) does not lend itself easily to analytical solution. For comparison purposes, f(t) can simply be a single sinusoid, such as

$$f(t) = F_o \cos \Omega t \tag{3.61}$$

Again using nominal values for the parameters and setting $F_o = 1.0$, the maximum amplitude predicted by the continuous model was $X_{max} = 0.39$ and the maximum amplitude computed from the discrete model was $X_{max} = 0.35$. This is a 10 percent difference in amplitudes.

Since it would be substantially more difficult to include nonlinearities or damping in the continuous model and the difference in the responses is fairly uniform and predictable for the range of variation of the input parameter vectors, it seems reasonable to adopt the discrete model. Neglecting the nonlinear effects and damping would most likely account for more error than neglecting the higher modes of vibration.

3.4 Nonlinearities and Damping

So that a comparison could be made with the continuous model, the discrete model has been idealized in two important ways--nonlinearities and damping. The dancer is supported by a pneumatic spring whose stiffness is highly nonlinear. The supports of the dancer also contain

friction. Damping is intentionally introduced to limit high frequency oscillations.

The stiffness of an air spring is treated in Thomson [11] and can be developed from the thermodynamic laws describing an isentropic process of an ideal gas. The stiffness of the pneumatic spring is determined to be

$$K_{ps} = \frac{nP_o A^2}{V_o}\left(1 - \frac{Ax}{V_o}\right)^{-(n+1)} \tag{3.62}$$

where

K_{ps} = air spring constant;

n = specific heat ratio (1.4 for air);

P_o = gas pressure at $x = 0$;

V_o = volume at $x = 0$;

A = piston area; and

x = displacement of the piston rod.

Friction and viscous damping are included in the dancer supports to reduce the motion and eliminate high speed chatter. The exact type of damping will vary from machine to machine. In an effort to generalize the frictional characteristics of the dancer supports, both linear and nonlinear damping are included. The nonlinear damping appears as a function of the dancer speed cubed. The frictional force is assumed to be

$$F_D = (b_1 + b_2\dot{x}^2)\dot{x} \tag{3.63}$$

where b_1 is the linear damping, b_2 accounts for the nonlinear effects, and $\dot{x}$ is the dancer velocity.

3.5 The Feedback System

The dancer's ability to accurately control the longitudinal tension as a passive device is severely limited by its own dynamics. Thus, the most effective use of the dancer is to use it as a tension sensing transducer in a control system. The dancer is an unusual transducer because it significantly influences the phenomenon which it measures.

The dancer can act as a transducer by moving about its equilibrium position in response to fluctuations in longitudinal web tension. As the web becomes slack or too taut, the dancer displaces accordingly to balance the spring and web forces acting on it. A signal, indicating the magnitude and direction of the dancer movement, is sent to the drive motor. The motor will increase or decrease the torque on the mill roll, and thus the web tension, until the dancer has moved back to its equilibrium position. At this point the machine should be operating at design conditions. For trim control, the ability of the dancer to change the speed of the web is limited to a certain percentage of the nominal value. For modeling purposes, this percentage is assumed to be 10 percent.

Figure 9 shows a block diagram illustrating the feedback system. The system consists of a gain amplifier to proportion the dancer signal, a field DC controlled motor, the dancer, and the gearing system. In the previous sections, the equations of motion for the dancer and web were derived. Dorf [12] derives the transfer function for a field driven motor relating the rotational speed to the field voltage as two cascaded first-order systems. One system consists of the mechanical elements of the motor and the second consists of the electrical field characteristics. Typically, the mechanical time constant is much larger than the

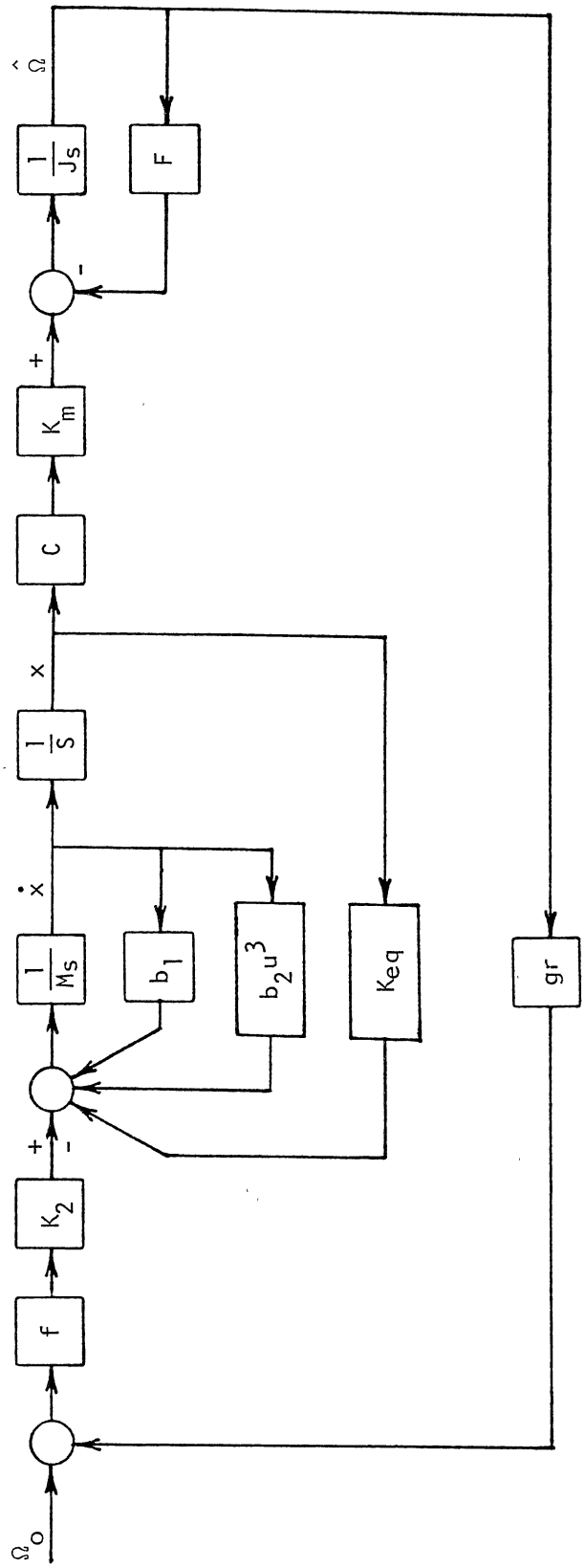

Figure 9. Block Diagram of Web, Dancer, and Feedback System

electrical time constant. Thus, the transfer function for the electric motor is

$$\frac{RS(s)}{V_f(s)} = \frac{K_m}{J_s + F} \tag{3.64}$$

where

RS = rotational speed of the motor;

V_f = field voltage;

K_m = motor constant;

J = effective inertia; and

F = viscous friction.

The inertia used in Equation (3.64) is the effective inertia of the system, which includes the inertia of the mill roll. The inertia of the mill roll can be related to the inertia of the motor through the gear ratio. The mill roll can be approximated as a homogeneous circular cylinder. The inertia and gear ratio are expressed as follows:

$$gr = \frac{\Omega_{motor}}{\Omega_{M.R.}} \tag{3.65}$$

$$J_{M.R.} = \frac{1}{2} mr^2 \tag{3.66}$$

$$J = J_{motor} + \frac{J_{M.R.}}{gr^2} \tag{3.67}$$

where m is the mass of the mill roll, r is the radius of the mill roll, and gr is the gear ratio.

All of the equations are written relative to nominal values of dancer position, web tension, field voltage, and rotational speed. The position of the dancer is related to the field voltage by a proportionality

constant which couples the equations of motion. This coupling makes control possible. The system is described by the subsequent equations:

$$f(t) = r - \sqrt{r^2 + e^2 + 2er\cos\omega t} - N\cos n\omega t \tag{3.68}$$

$$K_{ps} = \frac{n P_o A^2}{V_o}\left(1 - \frac{Ax}{V_o}\right)^{-(n+1)} \tag{3.69}$$

$$V_f = cx \tag{3.70}$$

$$M\ddot{x} + (b_1 + b_2 \dot{x}^2)\dot{x} + \left(K_{ps} + \frac{EA}{L_1} + \frac{EA}{L_2}\right)x = \frac{EA}{L_2} f(t) \tag{3.71}$$

$$J\dot{\hat{\Omega}} + F\hat{\Omega} = K_m V_f \tag{3.72}$$

$$\Omega = \Omega_o + gr(\hat{\Omega}) \tag{3.73}$$

3.6 Numerical Values

The model of the rewind portion of a web handling machine is presented in the previous section. This model contains many parameters which are unique to each web and winding machine. These quantities will make up the input parameter vector, discussed in more detail in Chapter IV, which are subject to the sensitivity analysis. Table I shows the parameters and their respective nominal values.

Much of the data in Table I was supplied by a local chemical company which operates machines handling polypropylene webs and through private communications with Dr. John J. Shelton, P.E. Items 2 through 14 are measured or estimated quantities from a winding machine handling a polypropylene web. The elastic information for polypropylene was located in Plastics Materials [13]. An approximate stress-strain curve

TABLE I

NOMINAL VALUES OF THE UNCERTAIN PARAMETERS

No.	Parameter	Nominal Value
1	Modulus of Elasticity	170,000 psi
2	Distance Between the Dancer and Mill Roll	110 in.
3	Distance Between the Dancer and Chill Roll	270 in.
4	Width	120 in.
5	Thickness	0.00075 in.
6	Dancer Mass	275 lbm
7	Pneumatic Spring Rate	27.5 lbf/in.
8	Linear Dancer Damping	15 lbf s/in.
9	Core Eccentricity	1.75 in.
10	Number of Nodes	6
11	Nodal Amplitude	0.75 in.
12	Line Speed	250 in./s
13	Radius	8.5 in.
14	Cubic Dancer Damping	0.1 lbf $s^3/in.^3$
15	Motor Inertia	0.025 lbf in. s^2
16	Motor Damping	1.75 lbf in.s
17	Feedback Gain	0.50 V/in.

indicated that the material is almost Hookian in its behavior until the yield strength is reached. The motor parameters are compliments of the Kollmorgen Corporation, Industrial Drives Division.

CHAPTER IV

SENSITIVITY ANALYSIS

The mathematical model developed in the previous chapter contains several uncertain parameters which limit the reliance that can be placed on the outcome of a single simulation. As a way of dealing with this problem, these quantities can be assigned statistical distributions which reflect their degree of parametric uncertainty. The outcome, now a function of random variables, is subject to statistical manipulation.

4.1 Classification of Model

The equations of the mathematical model can be rewritten as a set of first-order differential equations of the form

$$\dot{\underline{x}}(t) = f(\underline{x}(t), \underline{s}, \underline{u}(t)) \tag{4.1}$$

where $\underline{x}(t)$ is the state vector, $\underline{s}$ is the vector of parameters, and $\underline{u}(t)$ is the set of time-dependent function which include input or forcing functions.

The vector $\underline{s}$ consists of the inherent system parameters, initial state, and input variables which are uncertain. For specified $\underline{s}$, $\underline{u}(t)$, and $\underline{x}(o)$, $\underline{x}(t)$ is the solution of the system of equations and is a deterministic or a stochastic function of time as determined by the nature of $\underline{u}(t)$. Parameters from $\underline{s}$ are included in the forcing function $\underline{u}(t)$.

Each element of the vector $\underline{s}$ is defined as a random variable, the distribution of which is a measure of the uncertainty in the "real" but unknown value of the parameter. Thus, all the uncertainty is contained in the vector $\underline{s}$. Every sample of s taken from the a priori distributions results in a unique state trajectory, $\underline{x}(t)$.

A set of observed variables, $\underline{y}(t)$, calculated from the state vector is computed. Thus, for each randomly selected parameter set $\underline{s}_k$, there corresponds a unique observation vector $\underline{y}_k$ defining the behavior of the system. This behavior can be classified as an occurrence or nonoccurrence of some system behavior such as web tension. The behavior can now be thought of in a binary sense; either it occurs or it does not for a given parameter set $\underline{s}_k$.

4.2 Sensitivity Analysis

For a given behavior and set of parameter distributions $\underline{s}$, it is possible to explore the properties of the ensemble via computer simulation studies. In particular, a random choice of the parameter vector $\underline{s}$ from the predefined distributions leads to a state trajectory $\underline{x}(t)$, an observation vector $\underline{y}(t)$, and via the behavior-defining algorithm, to a determination of the occurrence or nonoccurrence of the behavior. A repetition of this process for many sets of randomly chosen parameters results in a set of sample parameter vectors for which the behavior was observed and a set for which the behavior was not observed. The basic ideas underlying the sensitivity analysis concern the degree to which the distributions of the observed behaviors and nonbehaviors separate.

Given a behavior B and parameter element s_i, if an individual distribution does not separate--that is, the cumulative distributions for

the occurrence and nonoccurrence behaviors are statistically identical--and if the induced covariance is small, then the parameter s_i, taken alone, appears to have no effect on the occurrence or nonoccurrence of the behavior. The behavior is insensitive to s over the multidimensional region of the parameter space defined by the a priori distributions.

A sensitivity ranking is based on a direct measure of the separation of the unknown continuous distributions for behaviors and nonbehaviors, $F(s_i,B)$ and $F(s_i,\bar{B})$, respectively, by employing the Kolmogorov-Smirnov two-sample test statistic

$$D_{m,n} = \sup_x | S_m(x) - S_n(x) | \tag{4.2}$$

where S_m and S_n are the sample distribution functions corresponding to $F(s_i,B)$ and $F(s_i,\bar{B})$ for m behaviors and n nonbehaviors. Since the number of samples from the parameter space is finite, S_m and S_n are estimates of the unknown continuous distributions $F(s_i,B)$ and $F(s_i,\bar{B})$, respectively. The statistic, $D_{m,n}$, is the maximum vertical distance between the occurrence and nonoccurrence distribution functions. Large values of $D_{m,n}$ indicate that the parameter is important in obtaining the behavior.

The Kolmogorov-Smirnov test statistic is nonparametric, so it is possible to assign a confidence measure to the estimate of the true distribution given only that it is continuous. Values of $D_{m,n}$, for which to accept the hypothesis that the two distributions are statistically identical, are presented in Table II.

One important property to notice about $D_{m,n}$ is that the number of samples required to estimate the separation of $F(s_i,B)$ and $F(s_i,\bar{B})$ is virtually independent of the number of parameters in the vector $\underline{s}$, since

TABLE II

VALUES OF THE KOLMOGOROV-SMIRNOV TWO-SAMPLE TEST STATISTIC AT WHICH TO ACCEPT THE HYPOTHESIS OF HOMOGENEITY BETWEEN SAMPLE DISTRIBUTIONS FOR M BEHAVIORS AND N NON-BEHAVIORS FOR VARIOUS CONFIDENCE LEVELS

Confidence Level (%)	Accept Homogeneity If
80	$D_{m,n} \leq 1.07 \sqrt{\frac{1}{m} + \frac{1}{n}}$
90	$D_{m,n} \leq 1.22 \sqrt{\frac{1}{m} + \frac{1}{n}}$
95	$D_{m,n} \leq 1.36 \sqrt{\frac{1}{m} + \frac{1}{n}}$
99	$D_{m,n} \leq 1.63 \sqrt{\frac{1}{m} + \frac{1}{n}}$

$D_{m,n}$ is a function only of the number of samples, m, leading to behaviors and the number of samples, n, leading to nonbehaviors. For more information concerning the uses and limitations of this method, the reader is referred to Young and Auslander [14].

4.3 Application of Methodology

The model defined by Equations (3.68) through (3.73) contains 17 system parameters as shown in Table I. The behavior for the model is defined in terms of dancer motion and the resulting tension in the web.

The motion of the dancer is obtained from the solution of the differential equations of motion. The critical span of the web occurs between the dancer and the rewind roll. Thus, the strain in the web is calculated by observing the relative motion of the ends of that span or, simply, the difference between the dancer motion and the displacement input. The resulting web stress is

$$\sigma_w = \frac{E}{L} [f(t) - x(t)] + \sigma_o \tag{4.3}$$

where σ_o is the stress due to the nominal longitudinal tension.

Because of the assumption concerning the stress distributions in the web and other factors not included in the model, such as temperature effects, permanent deformations will occur in the web before the stress reaches the yield strength. Thus, the behavior for the system is defined such that the stress in the web must not exceed 85 percent of the yield strength. This incorporates a modest but reasonable factor of safety to help guard against damage to the medium.

Examination of Equation (4.3) indicates that it is possible for the stress in the web to become negative, or compressive. Clearly, it does

not make sense to attempt to longitudinally compress a web. Also, the equations derived earlier were based on the assumption that the web does not become slack. The dynamics involved in dealing with a slack web, such as the whipping effect, are substantially more complex. For both simplicity and practical consideration, all negative stresses are considered to be nonacceptable system behaviors.

The dancer moves about its equilibrium position in response to the web and spring forces acting on it. However, the motion of the dancer is constrained by stops on the winding machine. This makes it possible for the dancer to "bottom out" on the stops. When this occurs, the dancer is no longer able to send accurate signals to the drive motor or provide adequate tension control. Since the dancer cannot operate as designed at this state, the bottom out condition is also defined as a nonbehavior. It is assumed that the dancer will bottom out at an amplitude of two inches.

In summary, for the output of the system to be classified as a behavior, the following equations must be true:

$$x_{max} < 2.0 \tag{4.4}$$

$$0 \leq \frac{\sigma_w}{S_y} \leq 0.85 \tag{4.5}$$

where S_y is the yield strength of the web.

4.4 Results of Application

Using Equations (4.4) and (4.5), a classification algorithm was written which categorized the output of each simulation as acceptable system behavior or not acceptable system behavior. The system was

simulated 500 times with randomly selected parameters. The classified result and corresponding parameter vector was stored. Of the 500 simulations conducted, 226 fell in the behavior category and 274 fell in the nonbehavior category. The Kolmogorov-Smirnov statistic, $D_{m,n} = 0.122$, indicates that $F(s_i,B) \neq F(s_i,\bar{B})$ at the 95 percent level of confidence. Table III contains the Kolmogorov-Smirnov test statistic for each parameter.

A ranking of the individual parameters on the basis of the test statistic classified 12 of the 17 parameters as unimportant for obtaining acceptable system behavior. It is essential to note that this result is only significant for the ranges of values in which the individual parameters were allowed to vary. For example, the radius of the mill roll may vary from 4 to 16 inches during the course of a run. However, permitting the corresponding parameter to vary 400 percent would necessitate a dramatic increase in the number of simulations needed to accurately investigate the region of uncertainty. Conversely, some parameters, such as the width, do not vary to a significant degree at any portion of a run. In an effort to not bias the statistical study for or against any parameter, nominal values (Table I) were chosen for each parameter and the interval limits were set at approximately 15 percent above and below this nominal value.

The five parameters found to be most significant to obtaining acceptable system response for the winding process are: modulus of elasticity, span length between the dancer and mill roll, thickness, core eccentricity, and number of nodes or bumps on the mill roll. The sample distribution functions under B and $\bar{B}$ for the important parameters are shown in Figures 10 through 14. The separation between the distribution

TABLE III

VALUES OF THE KOLMOGOROV-SMIRNOV
TWO-SAMPLE TEST STATISTIC FOR
EACH UNCERTAIN PARAMETER

No.	Parameter	$D_{m,n}$
1	Modulus of Elasticity	0.242
2	Distance Between the Dancer and Mill Roll	0.140
3	Distance Between the Dancer and Chill Roll	0.060
4	Width	0.060
5	Thickness	0.183
6	Dancer Mass	0.099
7	Pneumatic Spring Rate	0.064
8	Linear Dancer Damping	0.064
9	Core Eccentricity	0.146
10	Number of Nodes	0.200
11	Nodal Amplitude	0.078
12	Line Speed	0.071
13	Radius	0.041
14	Cubic Dancer Damping	0.083
15	Motor Inertia	0.058
16	Motor Damping	0.058
17	Feedback Gain	0.072

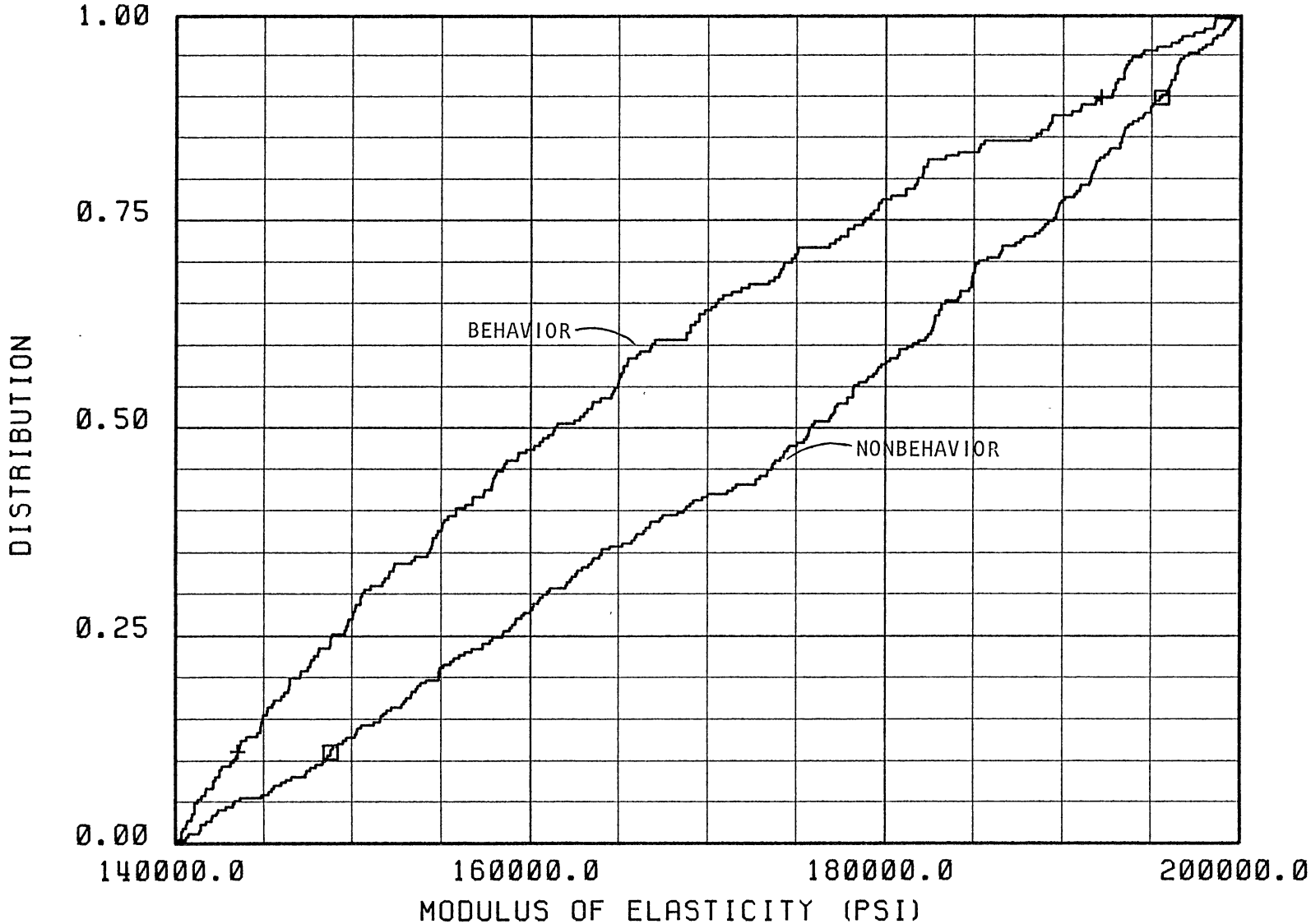

Figure 10. Sample Distributions for the Modulus of Elasticity of the Web

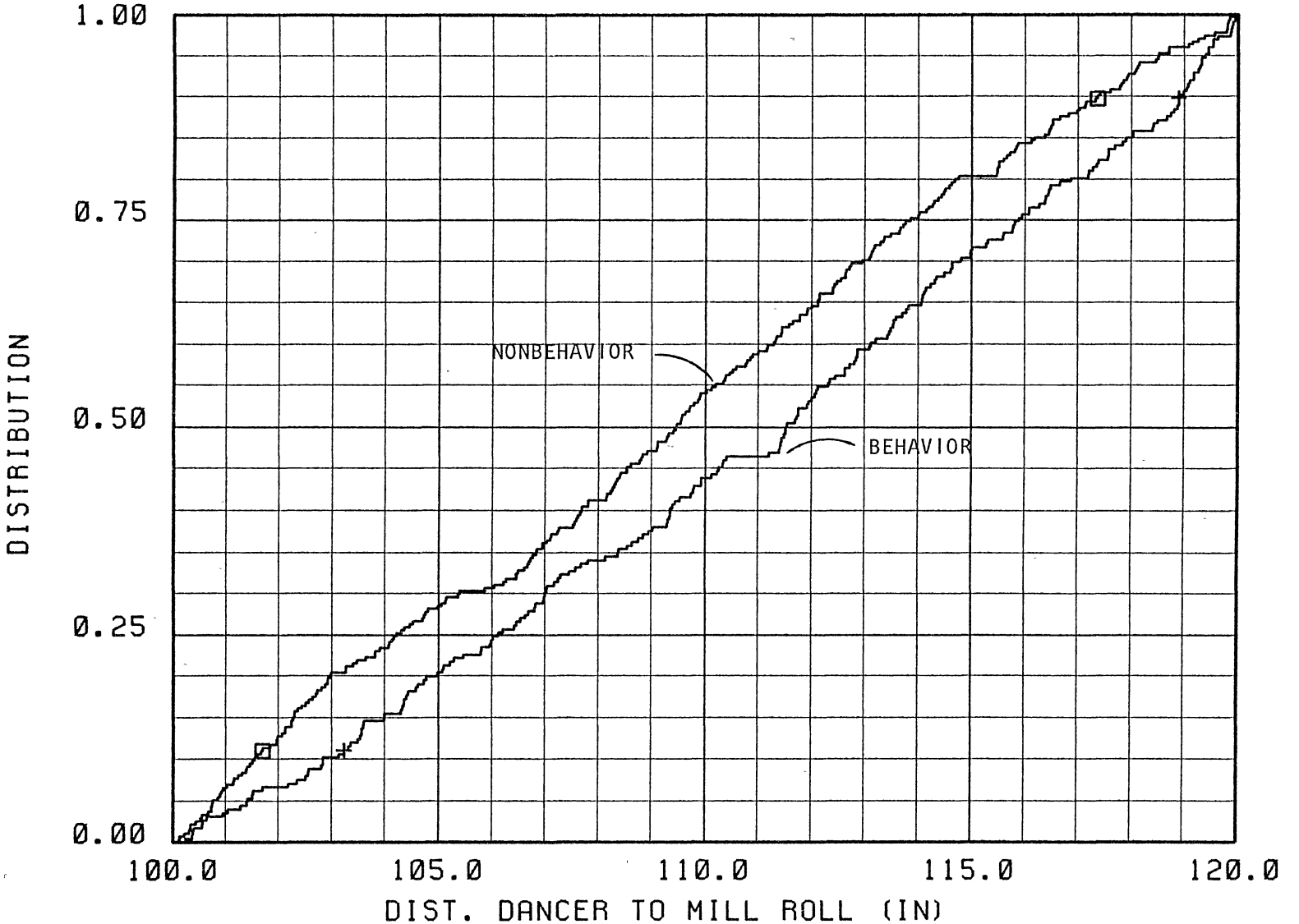

Figure 11. Sample Distributions for the Free Span Length Between the Dancer and Mill Roll

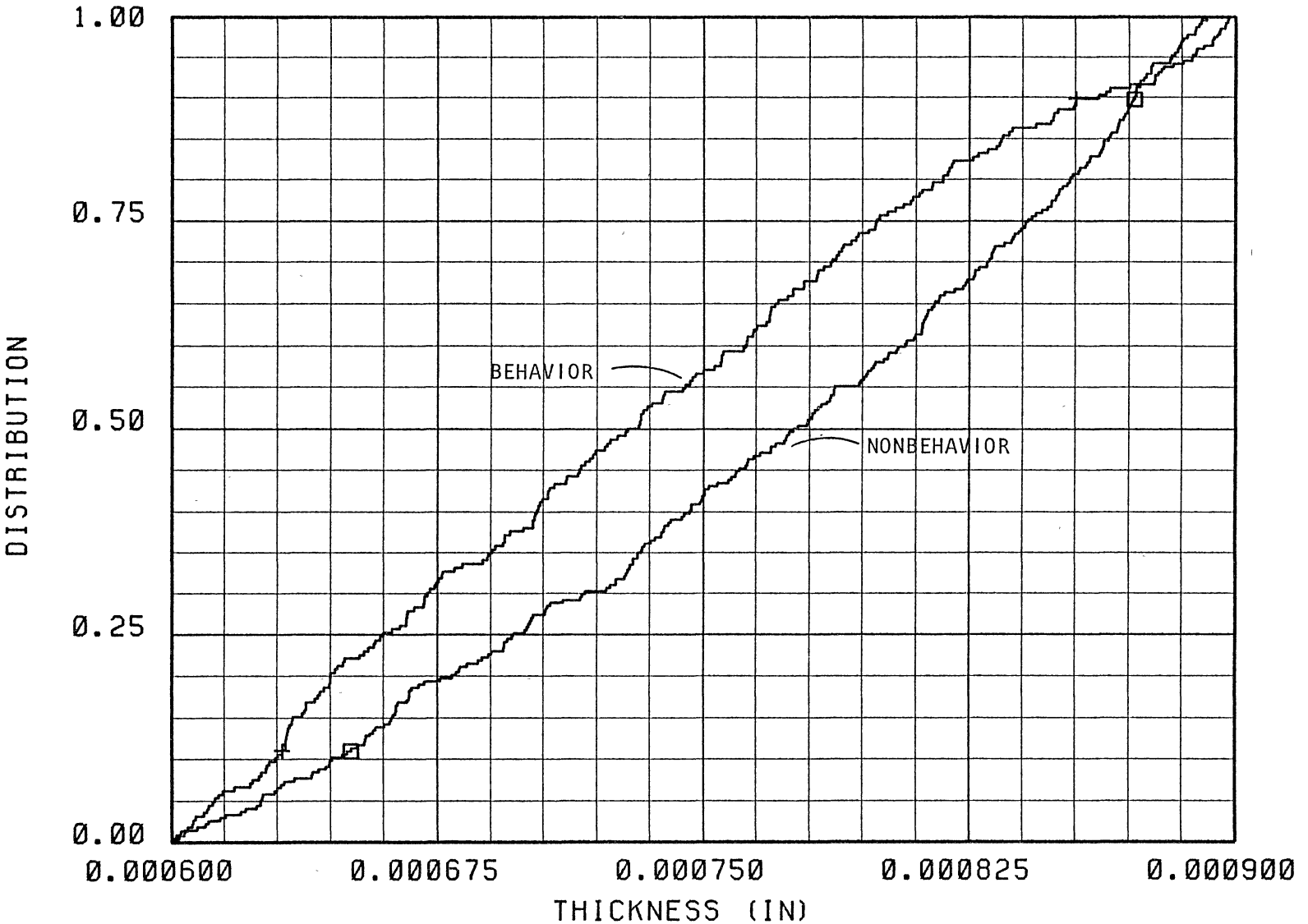

Figure 12. Sample Distributions for the Thickness of the Web

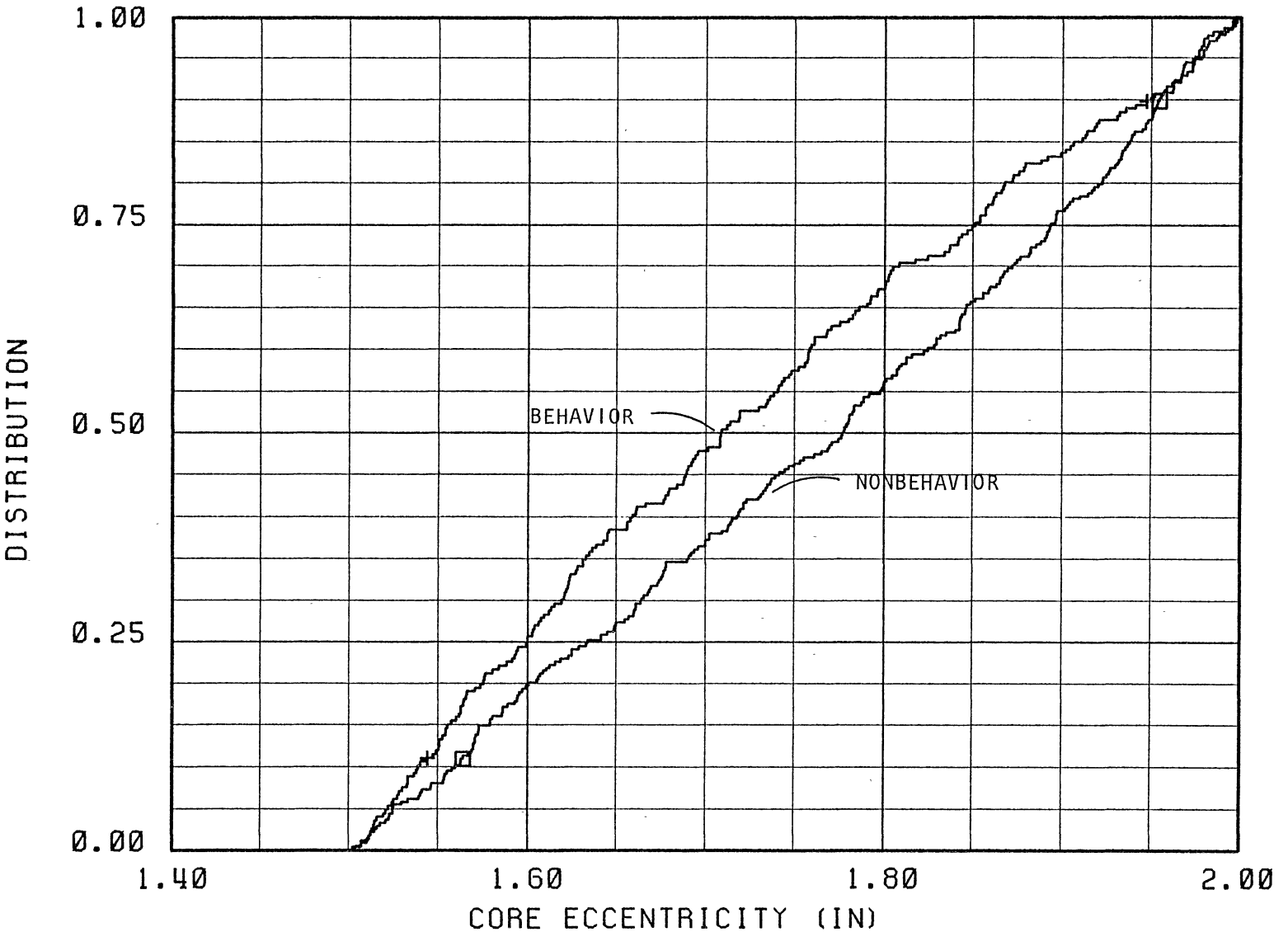

Figure 13. Sample Distributions for the Mill Roll Core Eccentricity

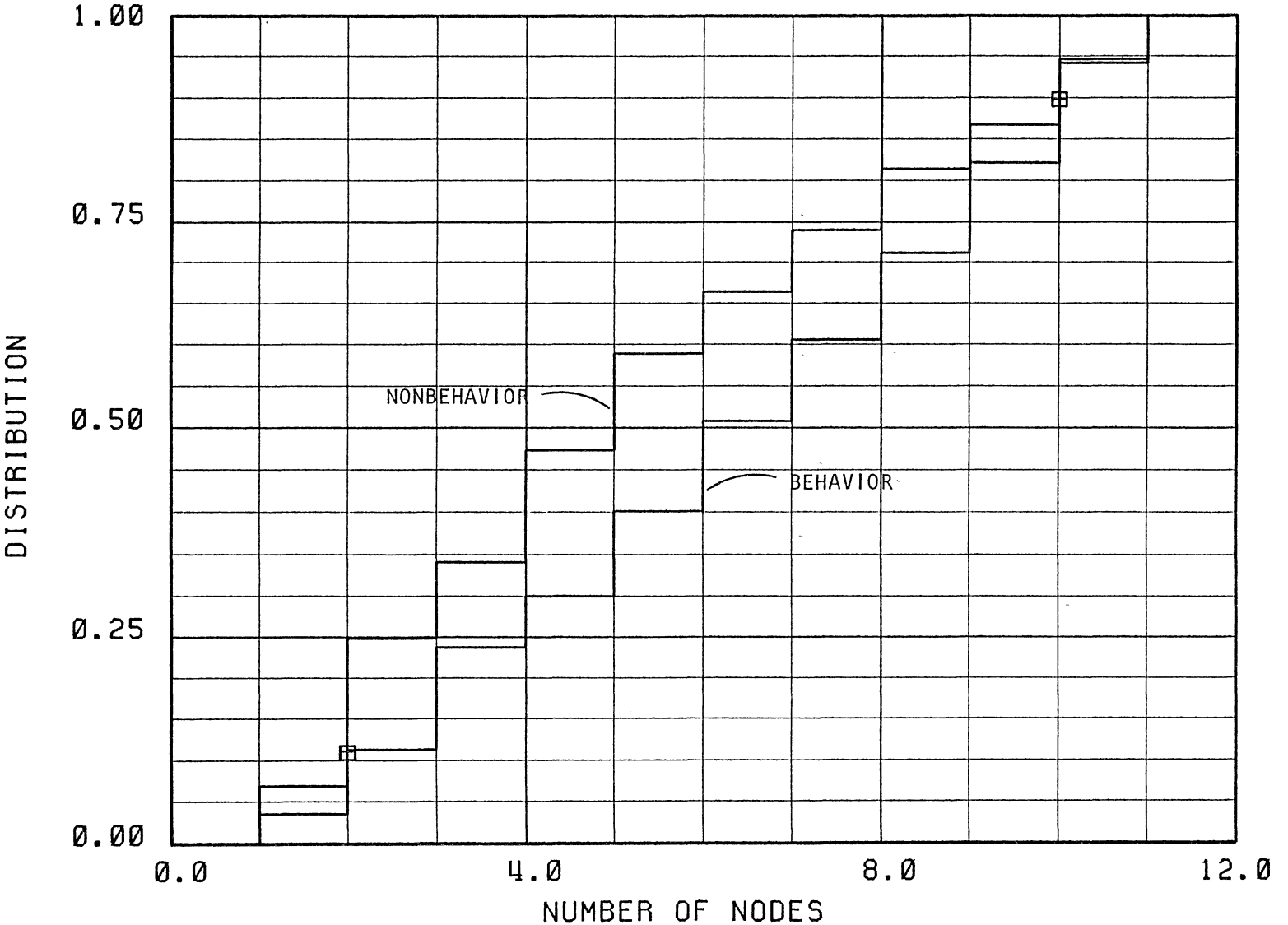

Figure 14. Sample Distributions for the Number of Nodes on the Mill Roll

functions, that is, the vertical distance between the curves, is the measure of the sensitivity of the model to the parameter in question.

For comparison purposes, the distribution functions for the motor inertia, $D_{m,n} = 0.058$, are presented in Figure 15. The small separation between the curves indicates that the motor inertia is not important to obtaining acceptable system response. This result is easily explained by examining the system. The motor inertia is unimportant because it is relatively small when compared to the large inertia of the mill roll. Thus, even a large change in the motor inertia will have little effect on the effective inertia used in the equations of motion.

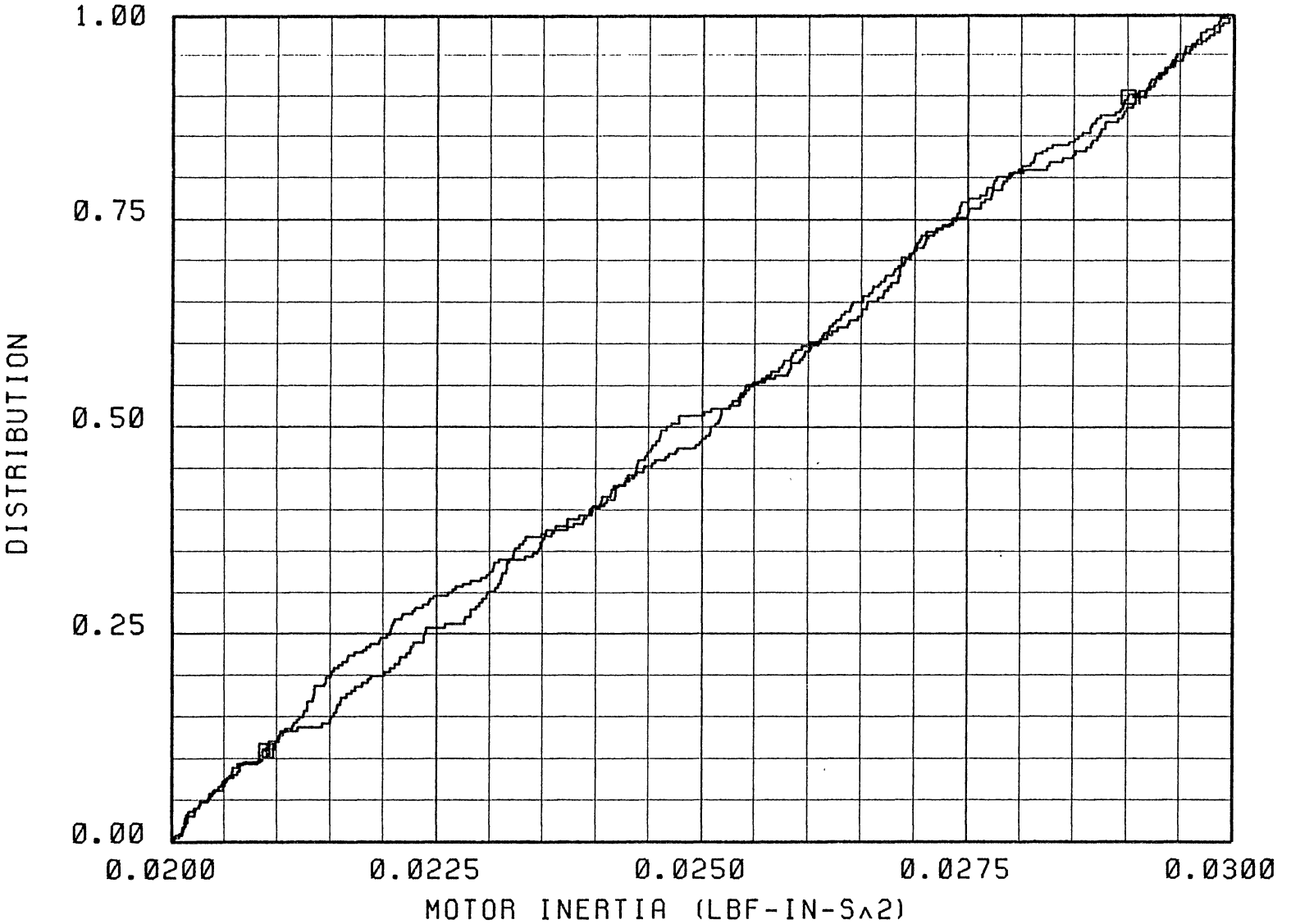

Figure 15. Sample Distributions for the Inertia of the Motor

CHAPTER V

CONCLUSIONS AND RECOMMENDATIONS

Based on the values of the Kolmogorov-Smirnov test statistic and shapes of the distribution functions, the importance of the parameters can be established. It is possible that the distributions of certain parameters will not separate under behavioral mapping and yet this parameter could be crucial to a successful simulation. This situation can occur when there exists a strong correlation among the parameters. Thus, the correlation coefficients must be computed for each parameter. These coefficients are a measure of the linear interaction between any two parameters.

It is important to note that the conclusions which follow are based on the ranges of the uncertainty for the parameters as shown in Table IV. It is likely that many of the parameters which are classified as insignificant could exercise greater influence on the outcome of a simulation if the limits of uncertainty were changed. The methodology of the sensitivity approach could be easily adapted to design work by defining ranges in which acceptable system behavior is assured. Hopefully, the conclusions of this thesis can provide direction to experimenters in the future. The parameters found insignificant should not be the subject of expensive or complicated testing procedures because they have little influence on the behavior of the system.

TABLE IV

RANGES OF UNCERTAIN PARAMETERS

No.	Parameter	Range
1	Modulus of Elasticity	140000.0-200000.0
2	Distance Between the Dancer and Mill Roll	100.0-120.0
3	Distance Between the Dancer and Chill Roll	245.0-295.0
4	Width	110.0-130.0
5	Thickness	0.0006-0.0009
6	Dancer Mass	250.0-300.0
7	Pneumatic Spring Rate	25.0-30.0
8	Linear Dancer Damping	10.0-20.0
9	Core Eccentricity	1.50-2.00
10	Number of Nodes	1.0-11.0
11	Nodal Amplitude	0.60-0.80
12	Line Speed	225.0-275.0
13	Radius	7.5-9.5
14	Cubic Dancer Damping	0.0-0.20
15	Motor Inertia	0.02-0.03
16	Motor Damping	1.60-1.90
17	Feedback Gain	0.00-1.00

5.1 Web Stiffness

Using the Kolmogorov-Smirnov test statistic, the modulus of elasticity, the free span length, and the web thickness are all classified as significant parameters (see Table II). Since the web is modeled as a longitudinal rod, the above parameters are directly related to the stiffness of the web, EA/L.

The distribution functions for the modulus of elasticity, Figure 10, show that the outcome of a simulation is more likely to be a behavior if the modulus is slightly less than nominal. This is determined by the slope of S_m, the sample distribution function corresponding to $F(s_i,B)$. The curves shown in Figures 10 through 15 are the integrals of the probability density functions. Thus, the greater the slope of the distribution function, S_m, the higher the probability of an occurrence. The converse is true for S_n, the sample distribution function corresponding to $F(s_i,\bar{B})$, and nonoccurrences. Since the slope of the S_m curve is greatest just below the nominal value of the elastic modulus while the S_n curve is shallowest in that region, the likelihood of an occurrence is greatest for values of the modulus of elasticity which are slightly less than nominal.

Examination of Figure 12 reveals that behaviors are more apt to occur at lower values of the thickness. Notice in both Figures 10 and 12 that the behavior curve lies above the nonbehavior curve, or for a given cumulative distribution, the corresponding values for behaviors are smaller than those for nonbehaviors.

The slopes for the behavior and nonbehavior curves in Figure 11 are not as conclusive as those in the figures for the elastic modulus and the thickness. However, the curve for behaviors is below the curve for non-

behaviors in Figure 11, which implies that slightly larger values of the free span length between the dancer and mill roll are more favorable to obtain an acceptable system response.

The observations for the modulus of elasticity, thickness, and free span length lead to a similar conclusion. The distributions suggest that a simulation is most likely to result in a behavior when the spring rate of the web, EA/L, is slightly less than nominal. This should not imply that continually lowering the web stiffness will continually increase the probability of behavioral response. It only means that for the ranges of the elastic modulus, thickness, and span length used in the simulations, acceptable system behavior occurred more often at stiffnesses less than nominal.

5.2 Frequency Ratio

The number of nodes on the mill roll determines the frequency of one component of the forcing function. The behavior curve in Figure 14 is above the nonbehavior curve, indicating that a higher input frequency will increase the probability of an occurrence. The nominal driving frequency, V/R, is approximately 1.7 times greater than the nominal natural frequency of the system. The ranges of the parameters involved in determining both the driving and natural frequencies cannot combine in such a way that the system is being driven at the resonant frequency.

The system could loosely be viewed as a mass-spring-damper system with base excitation. Thomson [11] indicates for systems with $\zeta = 0.5$ and the input frequency is 1.41 times greater than the natural frequency, the amplitude ratio is less than one, and the phase angle is less than 90 degrees. An increase in the frequency ratio, accomplished by lowering

the web stiffness or increasing the number of nodes on the mill roll, will reduce the amplitude ratio. The phase angle is important because if the motions of the ends of the web are out of phase, then f(t) and x(t) become additive. When this occurs, it is possible for a small input and small dancer motion to combine to sufficient magnitude to induce yielding in the web.

A limit exists on the amount that the stiffness and input frequency can be changed relative to one another. When the frequency ratio decreases, resonant behavior is observed. The resulting large values of strain will yield the web. On the other hand, as the frequency ratio increases, so does the phase angle. As the frequency ratio increases without bound, the phase angle tends toward 180 degrees and yielding of the web could occur.

5.3 Core Eccentricity and Nodal Amplitude

Figure 14 indicates the smaller core eccentricities will lead to more desired outcomes. The importance of the core eccentricity is a somewhat expected result. From Table I and Equation (2.1), it is clear that the core eccentricity is the principal component of the forcing function. Thus, the displacement input and resulting dancer motion are sensitive to the core eccentricity.

On the other hand, the sample distributions for the nodal amplitude failed to separate under behavioral mapping. Thus, the nodal amplitude was classified as insignificant in influencing the system response. There are two reasons why the nodal amplitude was categorized as insignificant. First, the excitation from the nodes occurs nominally at approximately ten times the natural frequency. Second, if the dancer is fixed, the

deflection caused by the nominal nodal amplitude is not sufficient to cause yielding in the web.

5.4 Influence of Other Parameters

The Kolmogorov-Smirnov statistic indicates that the dancer mass is not a significant parameter. The function of the dancer is twofold. Not only is it used to sense the web tension but also to help smooth out perturbations in the web. As a tension transducer, the dancer should be of low mass for fast response. A heavy dancer would smooth out perturbations more effectively. Thus, a compromise exists in selecting the dancer mass. The nominal value of the dancer mass is too large for the dancer to accurately transduce the tension but is too small to effectively smooth web perturbations. Thus, the model is insensitive to the dancer mass for the range of parametric uncertainty assumed in the simulations.

The mill roll radius and web line speed determine the input frequency of the forcing function. As noted earlier, the driving frequency, V/R, is 1.7 times greater than the natural frequency. The parameter ranges do not allow for the system to be driven at resonance. Since the forcing frequency cannot equal the resonant frequency for the given ranges of uncertainty, the results of the sensitivity analysis declaring the radius and line speed insignificant seem reasonable.

Assumptions were made in the development of the model that the dancer's maximum amplitude was two inches and its ability to change or trim the web speed was limited to ±10 percent from the nominal value. Both of these assumptions were used in obtaining the magnitude of the feedback gain. The nominal value and range for the gain does not allow the feedback system to adequately influence the winding operation. If the dancer

was allowed to trim more than 10 percent of the speed or if the control strategy was different, then the feedback system could be more influential in the outcome of a system simulation.

5.5 Cross Correlations

The correlations among the parameters were computed and all values of R and R^2 were sufficiently small as to indicate no linear correlation. This means that the variables do not sufficiently interact enough to increase or decrease the likelihood of an occurrence or nonoccurrence. Although the magnitude is small, it is interesting to note that the largest correlation occurred between the modulus of elasticity and the number of nodes.

The value of the correlation coefficient between the elastic modulus and the number of nodes is -0.213. The correlation is small because the amount that the stiffness and input frequency can change relative to one another and still produce acceptable behavior is limited as discussed in section 5.2. The negative correlation implies that a decrease in the elastic modulus and an increase in the number of nodes will increase the probability of the outcome of a simulation being classified as acceptable system behavior. This correlation could also be interpreted to imply that acceptable system behavior is likely when the number of nodes decreases and the elastic modulus increases. However, the observations made from inspecting Figures 10, 11, 12, and 14 indicate that this is not the case.

5.6 Recommendations for Future Work

Based on the conclusions stated above, it seems that the area of

most importance involves the stiffness of the web. A thorough testing of the web material in question in the form of stress-strain curves and yield strength calculations would be beneficial to future research and modeling work.

Another related area in which investigation would be invaluable is accurately defining the lateral stress profile across the web. Knowledge of the tension distribution would insure the validity of the one-dimensional representation of the web and provide guidance for selection of the factor of safety used in the critical stress calculations.

Further analytical and experimental investigation of the dynamics of a web would be significant. Two-dimensional dynamics and slack web dynamics were not discussed in this thesis but should be considered. Investigation of these areas may identify the causes of many mill roll defects as well as provide insight into the causes of wrinkles.

Further investigation into the types and applications of different control strategies would seem to be a worthy topic. The effect of increasing the dancer's trimming ability could also be investigated.

REFERENCES

[1] Altmann, H. C. "Formulas for Computing the Stresses in Center-Wound Rolls." TAPPI (April, 1968), pp. 176-179.

[2] Shelton, J. J. "Lateral Dynamics of a Moving Web." Ph.D. thesis, Oklahoma State University, Stillwater, Oklahoma, 1968.

[3] Shelton, J. J., and K. N. Reid. "Lateral Dynamics of an Idealized Moving Web." ASME Journal of Dynamic Systems, Measurement, and Control (Sept., 1971), pp. 187-192.

[4] Shelton, J. J., and K. N. Reid. "Lateral Dynamics of a Real Moving Web." ASME Journal of Dynamic Systems, Measurement, and Control (Sept., 1971), pp. 180-186.

[5] Blaedel, K. L. "Design Approach to Winding a Roll of Paper." Ph.D. thesis, University of Wisconsin, Madison, Wisconsin, 1974.

[6] Soong, T. C., and C. Li. "An Elastic Analysis of Multi-Roll Endless Web Systems." ASME Journal of Dynamic Systems, Measurement, and Control (Dec., 1979), pp. 308-314.

[7] Veits, V. L., I. Sh. Beilin, and V. M. Merkin. "Mathematical Models of an Elastic Strip in Mechanisms With Flexible Couplings." Applied Soviet Mechanics (Aug., 1983), pp. 721-726.

[8] Hornberger, G. M., and R. C. Spear. "An Approach to the Preliminary Analysis of Environmental Systems." Journal of Environmental Management (Dec., 1981), pp. 7-18.

[9] Timoshenko, S., D. H. Young, and W. Weaver. Vibration Problems in Engineering. New York: John Wiley & Sons, 1974.

[10] Meirovitch, L. Analytical Methods in Vibrations. New York: The Macmillan Company, 1967.

[11] Thomson, W. T. Theory of Vibration With Applications. Englewood Cliffs, N.J.: Prentice-Hall, 1981.

[12] Dorf, R. C. Modern Control Systems. Reading, Mass.: Addison-Wesley, 1981.

[13] Brydson, J. A. Plastics Materials. London: Butterworth Scientific, 1982.

[14] Young, G. E., and D. M. Auslander. "A Design Methodology for Nonlinear System Containing Parameter Uncertainty." Journal of Dynamic Systems, Measurement, and Control (March, 1984), pp. 15-20.

VITA

David Warren Plummer

Candidate for the Degree of

Master of Science

Thesis: MODELING AND SENSITIVITY ANALYSIS OF THE REWIND PORTION OF A WEB HANDLING MACHINE

Major Field: Mechanical Engineering

Biographical:

Personal Data: Born in Poteau, Oklahoma, June 2, 1962, the son of James W. and M. Joanne Plummer.

Education: Graduated from Memorial High School, Tulsa, Oklahoma, in May, 1980; received the Bachelor of Science degree in Mechanical Engineering from Oklahoma State University in May, 1984; completed requirements for the Master of Science degree at Oklahoma State University in December, 1985.

Professional Experience: Teaching Assistant, Department of Mechanical Engineering, Oklahoma State University, January, 1984, to May, 1985.